This paper is published as part of a themed issue of ***Photochemical & Photobiological Sciences*** containing papers from the

11th World Congress of the International Photodynamic Association

held in Shanghai, China, in March 2007

Guest edited by Kristian Berg and Qian Peng

Published in **issue 12, 2007** of ***Photochemical & Photobiological Sciences***.

Other papers in this issue:

Role of mitochondria in cell death induced by Photofrin®–PDT and ursodeoxycholic acid by means of SLIM†

Ingrid Kinzler, Elke Haseroth, Carmen Hauser and Angelika Rück*

Received 19th April 2007, Accepted 19th July 2007
First published as an Advance Article on the web 6th August 2007
DOI: 10.1039/b705919a

The present study was undertaken to find new ways to improve efficacy of photodynamic therapy (PDT). We investigated the combinatory effect of the photosensitizer Photofrin® and ursodeoxycholic acid (UDCA). UDCA is a relatively non-toxic bile acid which is used *inter alia* as a treatment for cholestatic disorders and was reported to enhance PDT efficiency of two other photosensitizers. Since besides necrosis and autophagic processes apoptosis has been found to be a prominent form of cell death in response to PDT for many cells in culture, several appropriate tests, such as cytochrome *c* release, caspase activation and DNA fragmentation were performed. Furthermore spectral resolved fluorescence lifetime imaging (SLIM) was used to analyse the cellular composition of Photofrin® and the status of the enzymes of the respiratory chain. Our experiments with two human hepatoblastoma cell lines revealed that the combination of Photofrin® with UDCA significantly enhanced efficacy of PDT for both cell lines even though the underlying molecular mechanism for the mode of action of Photofrin® seems to be different to some extent. In HepG2 cells cell death was clearly the consequence of mitochondrial disturbance as shown by cytochrome *c* release and DNA fragmentation, whereas in Huh7 cells these features were not observed. Other mechanisms seem to be more important in this case. One reason for the enhanced PDT effect when UDCA is also applied could be that UDCA destabilizes the mitochondrial membrane. This could be concluded from the fluorescence lifetime of the respiratory chain enzymes which turned out to be longer in the presence of UDCA in HepG2 cells, suggesting a perturbation of the mitochondrial membrane. The threshold at which PDT damages the mitochondrial membrane was therefore lower and correlated with the enhanced cytochrome *c* release observed post PDT. Thus enforced photodamage leads to a higher loss of cell viability.

Introduction

Photofrin® was the first photosensitizer approved by the US Food and Drug Administration (FDA) for photodynamic therapy (PDT) of palliative treatment of lung and esophageal cancer and for other disorders including Barrett's esophagus. The present status for the treatments of high-grade dysplasia in Barrett's esophagus and esophageal cancer, superficial bladder cancer, cholangiocarcinomas and advanced carcinoma of the lung are reviewed in the literature.[1–5] Photofrin® is a complex mixture of monomeric porphyrins and aggregates and cell death mechanisms depend on experimental conditions, such as drug and light dose, drug light interval and sensitivity of cells which may vary between different cell types.[6,7] Signs of apoptosis, as DNA fragmentation, caspase-3 and caspase-9 like activity and opening of the mitochondrial permeability transition pore complex (mPTPC) were found for example in a gastric cancer cell line by PDT with Photofrin®.[8] Apoptosis was also observed in CV-1 cells if they were irradiated 24 h after application of Photofrin®, whereas after only 1 h incubation, necrosis occurred.[9]

In general, the amount of apoptotic and necrotic processes depend on the photosensitizer and can be modulated by the incubation time (Fabris *et al.*[10]). Regulatory signalling pathways are activated in a photosensitizer, PDT dose and cell dependent fashion (recently reviewed by Agostinis *et al.*[11]). As also discussed by Oleinick *et al.*[12] photosensitizers that affect mitochondria are most efficient for inducing apoptosis following PDT. Examples are cationic lipophilic compounds but also negatively charged photosensitizers, such as Photofrin®, which is thought to bind to various cytosolic membranes and to mitochondrial constituents such as cardiolipins of the inner mitochondrial membrane,[13] or to the outer membrane peripheral benzodiazepine receptor (PBR).[14] It is known that porphyrins are endogenous ligands for the PBR, especially protoporphyrin IX (PPIX),[15] which is one of the main compounds of Photofrin®. Mitochondria are therefore thought to be important targets for inducing apoptosis in Photofrin® PDT. Already in 1997 Salet *et al.* could show in isolated rat mitochondria that photodynamic action leads to inactivation of the mitochondrial permeability transition pore which may lead to an impairment of the mitochondrial function.[16] The opening of the pore was regulated by conformational changes of the pore components.[17]

In an attempt to promote the efficacy of PDT with Photofrin®, this work investigated the effect of combining a drug which is not toxic, has been safely used for the treatment of a variety of gastric diseases and was described to enhance the phototoxicity of photosensitizers with predominant mitochondrial specificity. Among those drugs, Kessel *et al.*[18] have recently reported that

Institute for Lasertechnologies (ILM), Helmholtzstrasse 12, D-89081, Ulm. E-mail: angelika.rueck@ilm.uni-ulm.de

† Based on work presented at the 11th World Congress of the International Photodynamic Association in Shanghai, China, March 28–31, 2007.

ursodeoxycholic acid (UDCA) potentiates the apoptotic response to PDT with the porphycene photosensitizer CPO and tin etiopurpurin SnET2. UDCA is a hydrophilic dihydroxy bile acid which normally protects primary hepatocytes and hepatoma cells, as well as other cells from apoptosis induced by a variety of stimuli, as okadaic acid, hydrogen peroxide and ethanol.[19] UDCA is used clinically in a variety of cholestatic disorders,[20] as primary biliary cirrhosis, because it reverses the toxic effects of some hydrophobic bile acids.[21] It has become evident that the protecting effect is due to its ability to inhibit mitochondrial dysfunction by blocking the mPTPC[22] and inhibiting Bax translocation.[19] In contrast, UDCA significantly enhanced loss of mitochondrial potential, release of cytochrome *c* into the cytosol, activation of caspase-3 and apoptotic cell death after CPO and SnET2–PDT.[18] Since UDCA did not enhance the intracellular accumulation of the photosensitizers investigated, it was proposed that the mitochondrial membrane was sensitized to photodamage. Promotion of direct tumor cell kill by UDCA during SnET2–PDT could also be demonstrated in a radiation-induced fibrosarcoma tumor in the mouse.[23]

In the light of these findings, we assessed whether UDCA, currently used in gastroenterology for several indications, could be a safe and useful agent to promote PDT with Photofrin®. The role of mitochondria and the mitochondrial response to PDT was investigated in human hepatic cancer cells. Signs of mitochondrial induced apoptosis, as cytochrome *c* release and activation of caspase-3, -8 and -9 were followed up as well as other apoptotic markers. The subcellular distribution of Photofrin® was observed in the presence and absence of UDCA. Spectral resolved confocal fluorescence lifetime imaging (SLIM) was used to analyse the cellular composition of Photofrin®. In addition mitochondrial metabolism was studied by SLIM and correlated with signs of mitochondrial-induced apoptosis.

Materials and methods

Cell lines

The human hepatoblastoma cell line HepG2, expressing wild-type p53 protein was purchased from the American Type Culture Collection (ATCC HB-8065). Huh7 cells derived from a hepatocellular carcinoma, shown to express mutated p53[24] were generously given by Hubert Hug from the clinical department of paediatrics, University Ulm, Germany (present address: Dr. Hubert Hug, TheraSTrat AG, Allschwil, Switzerland). Both cell lines were maintained in RPMI 1640 medium (Gibco) supplemented with 10% FCS (Biochrom AG, Berlin, Germany) and 1% streptomycin–penicillin (Gibco/BRL). Cell lines were incubated in a humidified atmosphere at 37 °C and 5% CO_2.

Chemicals

The photosensitizer Photofrin® was a generous gift from Axcan Pharma Inc. (Mont-Saint-Hilaire, QC, Canada) as a freeze-dried powder. Photofrin® was freshly reconstituted before utilisation according to labelling and applied at a concentration of 2 μg ml^{-1} medium. The bile acid UDCA (99% purity) was also obtained from Axcan Pharma Inc. UDCA was dissolved in 0.2 M NaOH and applied at a 150 μM concentration. Recombinant protein molecular weight markers Cat. No. RPN 800 and RPN 756 were from Amersham Biosciences UK Ltd. (Bucks, UK).

The following kits were used: ApoAlert Cell Fractionation Kit (BD Clontech, Heidelberg, Germany), Suicide-Track™ DNA Ladder Isolation Kit (Calbiochem EMD Biosciences, Inc., La Jolla, CA, USA), and Biochrom-Gamma Kit (BIOCHROM AG seromed, Berlin, Germany).

Primary antibodies were: anti-caspase-3 (Cell Signaling Technology, Inc., Danvers, MA, USA) in a 1 : 1000 dilution, anti-caspase-8 (Apotech Corporation, Geneva, Switzerland) in a 1 : 1000 dilution, anti-caspase-9 (BD Biosciences Pharmingen, Heidelberg, Germany) in a 1 : 5000 dilution, cytochrome *c* antibody (included in ApoAlert cell Fractionation Kit) in a 1 : 100 dilution, anti-β-actin for loading control (Sigma, Saint Louis, Missouri, USA) in a 1 : 10 000 dilution.

Secondary antibodies were: goat-anti-rabbit IgG-HRP in a 1 : 5000 dilution, goat-anti-mouse IgG-HRP in a 1 : 5000 dilution, both obtained from Santa Cruz Biotechnology, Inc. (Santa Cruz, CA, USA).

Positive controls were: active recombinant human caspase-3 from Upstate Biotechnology, Inc. (Lake Placid, NY, USA), active recombinant human caspase-8 from BioVision Research Products (Mountain View, CA, USA), Camptothecin treated Jurkat lysate (BD Biosciences Pharmingen, Heidelberg, Germany) as a positive control for cleaved caspase-9.

All other chemicals were of analytical grade and obtained from standard commercial sources.

Viability assay

Cell viability was assessed using the neutral red assay[25] with Biochrom-Gamma Kit. For each sample, a 100 μl aliquot was transferred into a 96-well microtiter plate, and absorbance was measured at 570 nm (with a reference wavelength of 690 nm) on a multi-well reader (Lucy1, Anthos, Köln, Germany). The neutral red assay was verified concomitantly by trypan blue exclusion and counting the cells in a Neubauer-counting chamber.

Irradiation treatment and phototoxicity

The cytotoxicity of Photofrin® without light in the presence and absence of UDCA was first determined. Cells were incubated for 24 h with varying doses. Cytotoxicity was determined after washing the cells and re-incubating with fresh medium for another 24 h. Viable cells were determined by the viability assay. Cell survival was expressed as percentage of the non-treated controls.

For phototoxicity, cells were washed 24 h after incubation with the designated non-cytotoxic concentrations of Photofrin® and UDCA, then irradiated with varying light doses at 630 nm, emitted by a diode laser (Zeiss, Jena, Germany). The fluence rate was 100 mW cm^{-2}. Homogenous irradiation was achieved by a lens system. After irradiation cells were re-incubated with fresh medium for 48 h. During this time interval at least two divisions of the non-treated cells took place. The amount of the remaining viable cells was determined by the viability assay. The data herein presented were the results of at least three independent experiments. Cell viability was expressed as percentage of the untreated and non-irradiated control cells. For statistical evaluation, the mean value ± standard error of the mean (SEM) from 3 × 8 measurements was

calculated. Statistical calculations were done using the two-sided unpaired *t*-test. With a level of significance $\alpha = 0.05$, *T*-values $\geq$ 1.960 were considered significant.

Protein isolation and determination by western blot technique

For total protein isolation cells were harvested by detachment with 0.25% trypsin–0.1% EDTA in phosphate buffered saline (PBS) and pelleted by centrifugation (1500 rev min^{-1} for 5 min) followed by washing two times in ice-cold PBS. The pellet was re-suspended in lysis buffer and kept for 30 min on ice, then centrifuged for 15 min with 14 000 rev min^{-1} at 4 °C. Total protein concentration in the supernatant (*i.e.* the protein) was determined by the bicinchoninic acid method (bicinchoninic acid from Sigma, 4% copper(II) sulfate, Sigma, Sigma-Aldrich, Inc., St. Louis). Protein standard mixtures (Sigma) were used as references.

The protein samples were separated on discontinuous 10–20% SDS (sodium dodecyl sulfate) polyacrylamide gels (Zaxis International Inc., Hudson, OH, USA) or 4–20% polyacrylamide gels (Cambrex Bio Science Rockland, Inc., Rockland, MA, USA). Gels were loaded with 10 μg total protein per well for detection of the cytosolic fraction of cytochrome *c* and 50 μg protein for all other proteins. Equal loading was later on verified by reprobing the membranes with anti-β-actin. After electrophoresis proteins were transferred onto a nitrocellulose membrane (Hybond-ECL membrane from Amersham Biosciences UK Ltd.) by semidry electroblotting with the Panther™ Semidry Electroblotter device (Owl Separation Systems, Portsmouth, NH, USA). Membranes were blocked in 5% non-fat milk buffer and probed with the appropriate antibodies (see above). Antigen–antibody complexes were visualized with HRP-coupled secondary antibodies using the ECL™ western blotting detection reagents in combination with Hyperfilm™ ECL (Amersham Biosciences UK Ltd.).

Detection of cytochrome *c* release

Cytochrome *c* release from the mitochondria into the cytosol was measured as a sign of apoptosis. Cytosolic and mitochondrial fractions for cytochrome *c* detection were separated using the ApoAlert Cell Fractionation Kit at different times after treatment. The cytosolic fraction was examined by western blot technique.

DNA isolation and documentation of DNA fragmentation

DNA was extracted with the Suicide-Track™ DNA Ladder Isolation Kit according to procedure 1 of the instructions from the manufacturer, which allows at the same time separation of apoptic DNA from high molecular weight chromatin. DNA fragments ("laddering") were detected by electrophoresis in an agarose gel (1.5% agarose from GibcoBRL in Tris–borate–EDTA buffer). Gels contained 0.2 μg ml^{-1} ethidium bromide and were examined by UV illumination after electrophoresis. 50–2000 bp ladder molecular weight markers were used.

Measurement of cellular caspase-9, caspase-3 and caspase-8 activity

We tried to follow up activation of caspase-3, caspase-8 and caspase-9 at various times following treatment, by western blot technique. The antibody for caspase-3 recognizes the 30 kDa procaspase as well as the 17 kDa cleaving product, the antibody for caspase-8 the 57 kDa procaspase-8 as well as the 43, 41 and 18 kDa cleaving products, and the antibody for caspase-9 the 47 kDa procaspase-9 as well as the 37 and 35 kDa cleaving products. Functionality of antibodies was proved by using recombinant human caspases.

Time-resolved microscopy

In order to perform SLIM, a short pulsed diode laser emitting at 398 nm (PicoQuant GmbH, Berlin, Germany) was coupled to a laser scanning microscope (LSM410, Carl Zeiss, Oberkochen, Germany) *via* a coupling unit for external lasers and appropriate beam splitters. For SLIM the time-correlated-single-photon-counting (TCSPC) module 830/PML/16 (Becker & Hickl GmbH, Berlin, Germany) consisting on an ultra-fast 16 channel Hamamatsu R5900-01-L16 array and the TCSPC imaging module SPC-830 was attached to the microscope at the second descanned detection channel of the LSM410. The spectrograph MS125 (LOT-Oriel), with 600 lines mm^{-1} diffraction grating was coupled in front of the detector. The spectrometer was calibrated in a way, that a spectral range of approx. 200 nm could be detected with a spectral bandwidth of the channels of about 12 nm. The detailed experimental set-up has been previously published.[26] The TCSPC module receives the timing pulse from the laser and the scan clock signals (frame sync, line sync and pixel clock) from the scanning unit of the microscope.[27] For each photon, the TCSPC module determines the location within the scanning area, the time of the photon with respect to the laser pulse sequence and the detector channel number.

The detected image size was 128 × 128 pixel. The collimated laser beam for excitation was coupled into an objective (40× oil immersion, NA 1.30, Carl Zeiss, Oberkochen, Germany) and the fluorescence light was collected with the same objective and focused onto a pinhole, set to 100 μm corresponding to 5 Airy units in the focal plane. The images were recorded using a resolution of 1.25 μm $pixel^{-1}$. The pulse repetition rate of the diode laser was set to 40 MHz. Acquisition time for 128 × 128 pixel was 32 s. With the used zoom factor of 2 and a beam power of 120 μW for excitation an average irradiation of 60.4 J cm^{-2} was adjusted per acquisition time (it has to be mentioned that the 60.4 J cm^{-2} were applied during a scanning process with the ps diode laser at 398 nm as excitation source and that the biological response is not comparable to the phototoxicity induced during irradiation with the 630 nm cw diode laser). For curve acquisition 64 time channels were used. The fluorescence lifetime within the different spectral channels was calculated by a biexponential fitting routine using the SPCImage Version 2.8.3 software (Becker & Hickl GmbH). The fluorescence lifetime image was represented in pseudocolours.

Results

At first the cytotoxicity of Photofrin® was determined without light in presence and absence of UDCA. Cells were incubated for 24 h with varying doses. For Huh7 cells, Photofrin® alone was not toxic up to 5 μg ml^{-1} medium; UDCA was not toxic up to a concentration of 200 μM. HepG2 cells seemed to be more sensitive to Photofrin® (data not shown). In the combination, concentrations of 2 μg Photofrin ml^{-1} and 150 μM UDCA turned

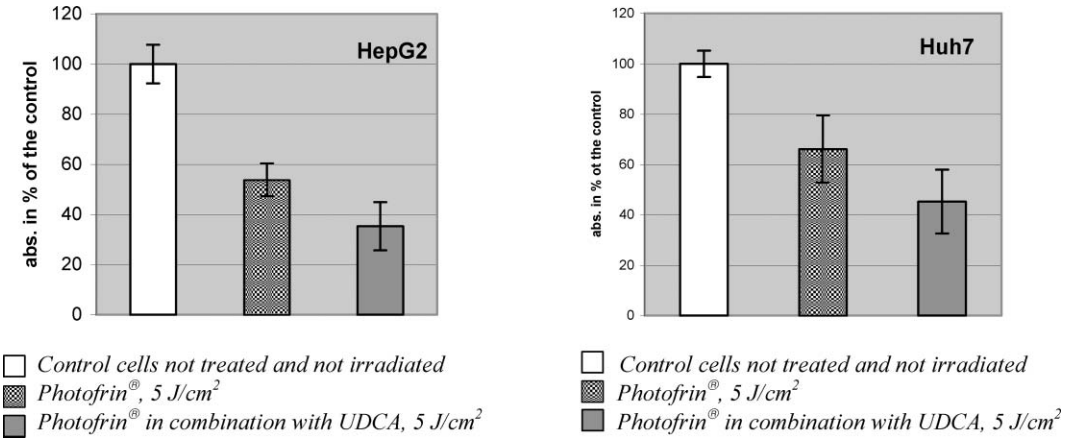

Fig. 1 Phototoxicity of 2 μg ml^{-1} Photofrin® in Huh7 cells (right) and HepG2 cells (left) in the absence and presence of 150 μM UDCA. Viability was measured 48 h after irradiation with 5 J cm^{-2} (see Materials and methods) as absorbance of neutral red compared to not treated control cells.

out not to be toxic for both cell lines (amount of viable cells >90%) and were subsequently used for the remaining experiments and for the evaluation of phototoxicity.

To determine phototoxicity, cells were irradiated with various light doses up to 10 J cm^{-2}. Fig. 1 demonstrates the results 48 h after irradiation with 5 J cm^{-2} where 50% of the HepG2 cells incubated with 2 μg ml^{-1} Photofrin® alone seemed to be viable (following the neutral red assay and hand counting). Under the same treatment conditions 65% of the Huh7 cells were still viable. This result is significantly different ($T = 3.419$) and probably reflects the fact that cells with mutated p53 gene are less sensitive to PDT.[28,29] Otherwise fluorescence investigation by laser scanning microscopy revealed one half of fluorescence intensity in Huh7 cells and thus lower accumulation of Photofrin (data not shown). Also at the higher light doses (data not shown) the HepG2 cells turned out to be more sensitive. When UDCA was concomitantly applied, the phototoxicity was significantly enhanced for both cell types ($T = 7.934$ for HepG2 and $T = 5.751$ for Huh7 cells).

In order to clarify the underlying molecular cell death mechanism cytochrome *c* release as a central event of apoptosis, activation of caspases and DNA fragmentation were investigated. Moreover, the cellular localization of Photofrin® and mitochondrial metabolism were analyzed by SLIM.

Cytochrome *c* release

Cytochrome *c* release into the cytosol at different times following irradiation with 5 J cm^{-2} is demonstrated in Fig. 2 for Huh7 and HepG2 cells. Whereas in the case of Huh7 cells (upper part (a)) a difference in cytochrome *c* release compared to the controls could not be observed independent of the treatment protocol, a significantly elevated release occurred for HepG2 cells (lower part (b)) incubated with Photofrin® 60 min post irradiation (lane 1). The cytochrome *c* release for cells incubated with Photofrin® in the presence of UDCA 60 min post irradiation was even more pronounced (lane 2). The signals were not yet as intense 30 min post irradiation but at this time the release was also more prominent when Photofrin® was applied in combination with UDCA (lane 3). Control cells, which were neither irradiated nor treated (lane 7), as well as treated cells but not irradiated (lane 6) and untreated cells irradiated only (lane 5) did show a marginal release.

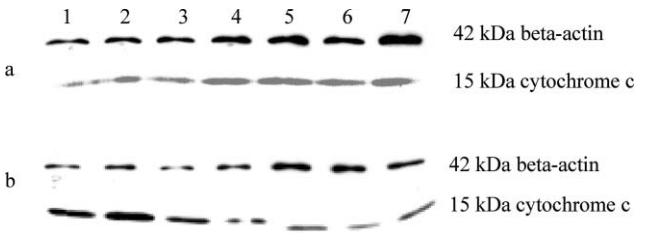

Fig. 2 Cytochrome *c* release in Huh7 cells (a) and HepG2 cells (b) with different treatment conditions: [1] cells incubated with 2 μg ml^{-1} Photofrin®, irradiation with 5 J cm^{-2}, 60 min post irradiation; [2] cells incubated with 2 μg ml^{-1} Photofrin® and 150 μM UDCA, irradiation with 5 J cm^{-2}, 60 min post irradiation; [3] cells incubated with 2 μg ml^{-1} Photofrin® and 150 μM UDCA, irradiation with 5 J cm^{-2}, 30 min post irradiation; [4] cells incubated with 2 μg ml^{-1} Photofrin®, irradiation with 5 J cm^{-2}, 30 min post irradiation; [5] cells irradiated with 5 J cm^{-2}; [6] cells incubated with 2 μg ml^{-1} Photofrin® and 150 μM UDCA, no irradiation; [7] control cells not incubated and not irradiated.

Caspase-3

We investigated the caspase-3 activation in short time intervals up to 60 min and in addition at 90, 120 and 150 min post PDT. Although procaspase-3 was expressed in both cell lines as shown in Fig. 3 and 4 we never detected active cleaved caspase-3 within the used time intervals irrespective of all treatment conditions that were applied. Also there was no attenuation of the procaspases to be seen which could have been an indirect sign of cleavage. This was equally true for the expressions of caspase-8 and -9 which were investigated under the same treatment conditions (data not shown). As an example, western blots of caspase-3 are demonstrated in Fig. 3 (Huh7 cells) and Fig. 4 (HepG2 cells) for 90, 120 and 150 min post PDT. Data for short time intervals up to 60 min are not shown.

DNA fragmentation

Major DNA fragmentation being one of the main hallmarks and a late event in apoptosis was examined at 60 and 120 min and at 3.5 and 4 h post irradiation. The result was different for both cell lines. As shown in Fig. 5(a) there was no "laddering" to be seen at all times investigated for Huh7 cells whereas the typical laddering was detected for HepG2 beginning at 3.5 h post

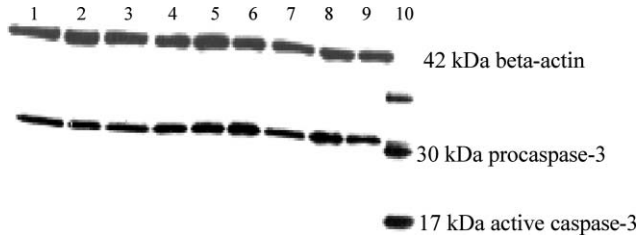

Fig. 3 Caspase-3 in Huh7 cells under different treatment conditions: [1] control cells, not treated and not irradiated; [2] cells incubated with 2 μg ml^{-1} Photofrin® and 150 μM UDCA; [3] cells with irradiation only; [4] cells incubated with 2 μg ml^{-1} Photofrin®, 90 min post irradiation with 5 J cm^{-2}; [5] cells incubated with 2 μg ml^{-1} Photofrin® and 150 μM UDCA, 90 min post irradiation with 5 J cm^{-2}; [6] same as [4] but 120 min post irradiation; [7] same as [5] but 120 min post irradiation; [8] same as [4] but 150 min post irradiation; [9] same as [5] but 150 min post irradiation; [10] positive control = active recombinant caspase-3.

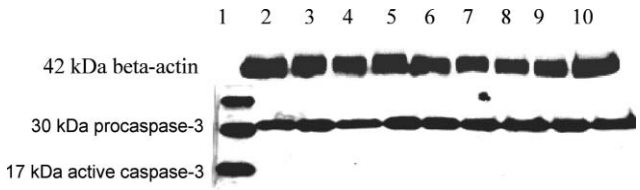

Fig. 4 Caspase-3 in HepG2 cells under different treatment conditions: [1] positive control = active recombinant caspase-3; [2] untreated and not irradiated control cells; [3] cells incubated with 2 μg ml^{-1} Photofrin® and 150 μM UDCA; [4] cells with irradiation only; [5] cells incubated with 2 μg ml^{-1} Photofrin®, 90 min post irradiation with 5 J cm^{-2}; [6] cells incubated with 2 μg ml^{-1} Photofrin® and 150 μM UDCA, 90 min post irradiation with 5 J cm^{-2}; [7] same as [5] but 120 min post irradiation; [8] same as [6] but 120 min post irradiation; [9] same as [5] but 150 min post irradiation; [10] same as [6] but 150 min post irradiation.

irradiation (Fig. 5(b)), for cells which were treated in the absence of UDCA (lane 6). Marginal signs of laddering were also observed in control cells and cells treated with Photofrin–PDT in the presence of UDCA.

Time resolved microscopy

In order to observe the subcellular distribution and analyze the molecular composition of Photofrin® in the presence and absence of UDCA, SLIM was performed. The fluorescence lifetime was analyzed in different spectral channels between 500 and 700 nm. The spectrometer was calibrated in a way, that the spectral bandwidth of the channels was about 12 nm. Fig. 6 demonstrates SLIM of HepG2 cells incubated 24 h with 2 μg ml^{-1} Photofrin® within a spectral range between 639–651 nm, which coincides with the fluorescence of mainly monomeric porphyrins.

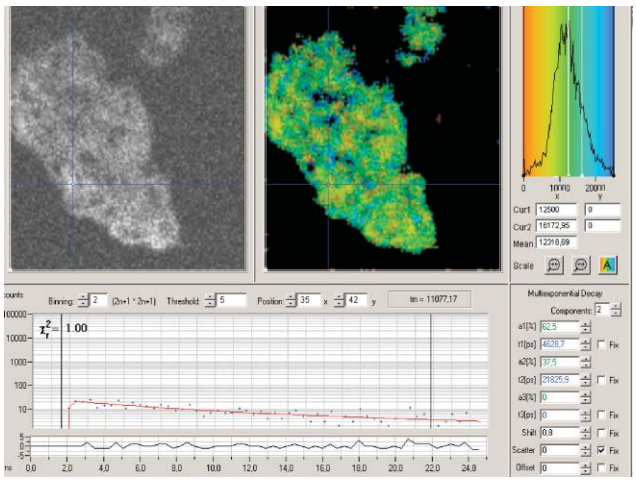

Fig. 6 SLIM of HepG2 cells incubated 24 h with 2 μg ml^{-1} Photofrin®. The gray image shows the fluorescence intensity, the color image the fluorescence lifetime within the spectral range 639–651 nm. On the right is the mean fluorescence lifetime distribution within the whole area of measurement. The graph represents the measured photons (blue curve) and the fitted curve (red) of the indicated pixel, after biexponential fitting. Approximately 20 cells are seen on the screen.

The fluorescence was excited with a ps diode laser at 398 nm. The fluorescence lifetime image is represented in false colors. On

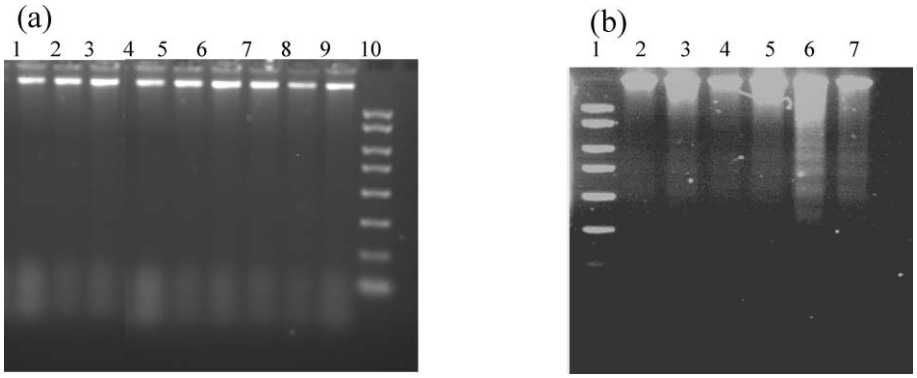

Fig. 5 Major DNA fragmentation: (a) Huh7 cells under different treatment conditions: [1] cells incubated with 2 μg ml^{-1} Photofrin®, 60 min post irradiation with 5 J cm^{-2}; [2] cells incubated with 2 μg ml^{-1} Photofrin® and 150 μM UDCA, 60 min post irradiation with 5 J cm^{-2}; [3] same as [1] but 120 min post irradiation; [4] same as [2] but 120 min post irradiation; [5] same as [1] but 3.5 h post irradiation; [6] same as [2] but 3.5 h post irradiation; [7] same as [1] but 4 h post irradiation; [8] same as [2] but 4 h post irradiation; [9] control cells, not treated and not irradiated; [10] DNA marker, the 8 bands represent DNA sizes from 50 to 2000 base pairs. (b) HepG2 cells under different treatment conditions: [1] DNA marker; [2] control cells, not treated and not irradiated; [3] cells incubated with 2 μg ml^{-1} Photofrin®; [4] cells incubated with 2 μg ml^{-1} Photofrin® and 150 μM UDCA; [5] cells with irradiation only; [6] cells incubated with 2 μg ml^{-1} Photofrin®, 3.5 h post irradiation with 5 J cm^{-2}; [7] cells incubated with 2 μg ml^{-1} Photofrin® and 150 μM UDCA, 3.5 h post irradiation with 5 J cm^{-2}.

the left side the image intensity is demonstrated in gray scales. The lower graph represents the measured photon counts within the indicated pixel (blue curve) and the fitted curve (in red) obtained by a biexponential fitting routine, which was proved to yield the best fit. The histogram with the mean lifetime distribution and color-coding is shown on the upper right. The maximum mean lifetime concluded from the histogram was 12.5 ns, which was mainly found in the cytoplasm of the cells. A lifetime between 11 and 14 ns was correlated with monomeric porphyrins.[30] The fluorescence quantum yield of porphyrins is quite low, therefore binning was set to 2; that means, that the lifetime was calculated as the mean of a 5 × 5 pixel area which reduced spatial resolution. HepG2 cells grow in clusters (see Fig. 6), which renders subcellular detection of SLIM more difficult. Nevertheless, we were able to differentiate between various species and metabolites of Photofrin® (see below).

SLIM was also performed for cells, incubated with Photofrin® in the presence of UDCA. Fig. 7 demonstrates SLIM of HepG2 cells, treated 24 h with 2 μg ml^{-1} Photofrin® and 150 μM UDCA in the spectral range 639–651 nm.

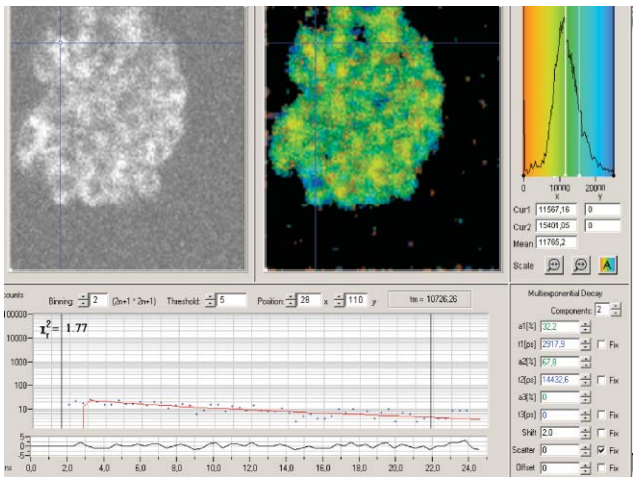

Fig. 7 SLIM of HepG2 cells incubated 24 h with 2 μg ml^{-1} Photofrin® and 150 μM UDCA. The gray image demonstrates the fluorescence intensity, the color image SLIM within the spectral range 639–651 nm. On the right is the fluorescence lifetime distribution within the whole area of measurement. The graph represents the measured photons (blue curve) and the fitted curve (red) of the indicated pixel, after biexponential fitting. Approximately 20 cells are seen on the screen.

Compared to HepG2 cells incubated with Photofrin® alone, the fluorescence intensity increased and the lifetime decreased. The maximum mean lifetime concluded from the histogram was 11.6 ns compared to 12.5 ns without UDCA, which mainly coincides with monomers.

Fig. 8 demonstrates SLIM of HepG2 cells, incubated with Photofrin® and UDCA within different spectral ranges. The same color-coding was used for all images. Different compounds of Photofrin® could be distinguished. The lifetimes in the channels between 687–699 nm and between 627–639 nm, were more or less in the same order, as seen from the color and the maximum mean lifetime of the histogram (12.9 and 12.7 ns, respectively). The lifetime distribution between 663–675 nm was however significantly different (see color change) and the maximum lifetime was shifted towards shorter values (around 8 ns). As known from fluorescence spectroscopy of Photofrin® and other porphyrins[31] the spectral range between 627–639 nm coincides with the main fluorescence band of monomeric protoporphyrin IX and hematoporphyrin, whereas the spectral range between 687–699 nm coincides with the second fluorescence band of the same molecules. In contrast, the spectral range between 663–675 nm belongs to aggregates and photoproducts of Photofrin®. Consequently, the lifetimes were shifted towards shorter values around 8 ns in agreement with our previous reports.[32]

Fig. 8 also demonstrates the spectral range between 508 and 520 nm. This fluorescence coincides with the autofluorescence of the cells, mainly originated from the enzymes of the respiratory chain, *i.e.* flavin molecules. The lifetime was significantly shorter; a biexponential fit delivered a value around 6 ns, a value which was also found by Schneckenburger and König.[33]

In addition to HepG2, Huh7 cells were incubated 24 h with 2 μg ml^{-1} Photofrin® in presence and absence of 150 μM UDCA. The fluorescence lifetime was calculated within different spectral ranges. The fluorescence intensity of Photofrin® was found to be approximately one half of that found for HepG2 cells, which could explain the slightly decreased phototoxicity of Huh7 cells (see Fig. 1). Table 1 summarizes the lifetimes of HepG2 and Huh7 cells which were not incubated (control cells), incubated with Photofrin® or UDCA alone or incubated with the combination. The lifetimes within different spectral ranges were calculated from at least 6 independent measurements (6 different images) together with the standard deviation as mean of the maximum lifetime, obtained from the histogram of the lifetime distribution. Statistical calculations were done using the two-sided unpaired *t*-test. With a level of significance $\alpha = 0.05$, T-values ≥ 2.969 were considered significant.

As can be concluded from Table 1, the lifetimes of Photofrin® did not change significantly in the absence or presence of UDCA (range 627–639 nm and 651–663 nm). Control cells as well as cells incubated only with UDCA did not show any fluorescence in the red spectral range.

The lifetimes of monomeric porphyrins (spectral range 627–639 nm, Table 1) were statistically not different for HepG2 and Huh7 cells ($T = 1.934$ for cells incubated with Photofrin®

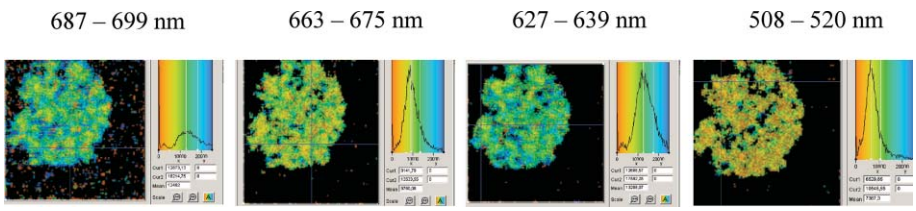

Fig. 8 SLIM of HepG2 cells incubated 24 h with 2 μg ml^{-1} Photofrin® and 150 μM UDCA, demonstrated within different spectral ranges.

Table 1 Maximum fluorescence lifetime and standard deviation of HepG2 and Huh7 cells measured within different spectral ranges. Standard deviation is from at least 6 independent measurements

HepG2 cells			
	Range 508–520 nm	Range 627–639 nm	Range 651–663 nm
Control	4.7 ± 0.4 ns		
UDCA	4.9 ± 0.5 ns		
Photofrin®	5.2 ± 0.9 ns	13.3 ± 0.6 ns	8.0 ± 0.6 ns
Photofrin® + UDCA	6.4 ± 0.6 ns	12.8 ± 0.7 ns	8.0 ± 0.5 ns
Huh7 cells			
	Range 508–520 nm	Range 627–639 nm	Range 651–663 nm
Control	8.6 ± 0.4 ns		
UDCA	8.6 ± 0.8 ns		
Photofrin®	9.2 ± 0.6 ns	11.8 ± 1.6 ns	9.4 ± 0.6 ns
Photofrin® + UDCA	8.4 ± 0.3 ns	11.9 ± 0.9 ns	9.6 ± 0.4 ns

alone and $T = 2.15$ when UDCA was present), indicating that subcellular localization was the same, irrespective of the presence of UDCA. However, the lifetime of aggregates and photoproducts was significantly different for HepG2 and Huh7 cells (spectral range 651–663 nm, Table 1) with a shorter lifetime for HepG2 ($T = 4.0415$ for cells incubated with Photofrin® alone and $T = 6.1207$ when UDCA was present). This might reflect presence of aggregates and enhanced formation of photoproducts in HepG2 cells, developing during laser scanning microscopy.

It was proposed that UDCA promotes photosensitizer binding to the mitochondrial membrane.[18] Therefore the role of mitochondria and mitochondrial response was of main interest in our study. Mitochondrial metabolism was studied by measuring the fluorescence lifetime of the autofluorescence. Important enzymes of the respiratory chain, which give rise to autofluorescence signals in the green spectral range are coenzymes of flavoproteins. The constituents are flavine mononucleotide (FMN) and flavinadenine dinucleotide (FAD) with the fluorescent prosthetic group isoalloxazine. It is known, that the lifetime of free unbound isoalloxazine in oxidized FMN is between 5–6 ns,[33] whereas in flavoproteins the lifetime is a complex mixture of very short components.[34] It is also known, that within a deficient respiratory chain, the concentration of oxidized FMN increases.[35] Therefore, the fluorescence lifetime gets probably longer due to uncoupling of the respiratory chain, leading to a higher amount of unbound isoalloxazine. The lifetime of the autofluorescence in respiratory deficient saccharomyces was detected between 8 and 10 ns.[36]

As can be seen in Table 1 the lifetime in the spectral range between 508–520 nm was significantly different for HepG2 and Huh7 cells ($T = 7.3$ for cells incubated with Photofrin® and UDCA). It seems that the mitochondrial metabolism is different for the two cell lines, whereby the Huh7 cells demonstrated a lifetime similar to that of respiratory deficient saccharomyces[36] even in control cells. Also Huh7 cells did not show enhanced cytochrome *c* release following PDT or signs of apoptosis as DNA laddering (see Fig. 2(a) and 5(a)).

For HepG2 we found that the fluorescence lifetime of flavines was significantly longer when cells were incubated with Photofrin® in presence of UDCA compared to control cells or cells incubated with UDCA alone ($T = 5.7746$ control/Photofrin® + UDCA, $T = 4.7044$ UDCA/Photofrin® + UDCA). Cells incubated with Photofrin® alone were not significantly different from control cells and cells incubated with UDCA alone. The lifetimes of cells incubated with Photofrin® + UDCA and Photofrin® alone were different, however due to the high standard deviation of Photofrin incubated cells the result seems not to be statistically different ($T = 2.7175$; $T \geq 2.969$ is considered significant). Nevertheless the result indicates enhanced perturbation of the mitochondrial membrane induced by Photofrin when UDCA is present causing enhanced phototoxicity with cytochrome *c* release during PDT (see Fig. 1 and 2).

Discussion

Strategies to evaluate new indications for PDT and to enhance efficacy of PDT are currently developed. In 2000 hydrophilic UDCA was reported by Kessel *et al.* to induce apoptosis in hepatocellular carcinoma cells and to potentiate PDT of CPO and SnET2,[18] two photosensitizers which catalyze mitochondrial photodamage. UDCA potentiated the loss of mitochondrial potential, release of cytochrome *c* into the cytosol and activation of caspase-3. However, UDCA has been also described as decreasing apoptosis *via* modulation of mitochondrial function by inhibiting mitochondrial membrane depolarization and cytochrome *c* release in hepatic and nonhepatic cells.[37,22] In contrast, only recently UDCA was found to enhance HepG2 cell toxicity of the hydrophobic bile acid chenodeoxycholic acid (CDCA) by diverging apoptosis to necrotic pathways.[38] Thus, the role of UDCA in hepatic apoptosis is controversial.

In this work the combinatory effect of Photofrin®–PDT and UDCA was investigated in two human hepatoma cell lines. A special attempt was made to characterize the involvement of mitochondria in the process. It was reported, that after a prolonged incubation (16 h and more) Photofrin® localized into the intracellular membranes including mitochondria.[39] Within our work, Photofrin® alone and in combination with UDCA were incubated for 24 h and applied in concentrations which were by themselves not toxic for both cell lines. From our findings UDCA significantly enhanced the PDT efficiency of Photofrin®. The enhancement was correlated with an increased cytochrome *c* release from the mitochondria into the cytosol following PDT in the case of HepG2 cells (see Fig. 2). In contrast, no increased release could be observed for Huh7 cells. Although cytochrome *c* release is a sign of apoptosis no caspase-3 activation could be detected within the used time intervals by means of western blot technique and this was true for both cell lines. Also activation of caspase-8 and caspase-9 could be excluded by western blot technique. Therefore, we had to address the question whether the mechanism of Photofrin® and Photofrin®/UDCA induced cell death is triggered by apoptosis at all. As a test therefore we chose the detection of major (= stage II) DNA-fragmentation which degrades DNA into pieces of approximately 180 bp. The result was different for both cell lines. In HepG2 cells we could detect the typical "laddering" beginning at 3.5 h post irradiation, whereas in the case of Huh7 cells, no laddering was observed (see Fig. 5(a) and (b)). Therefore we can conclude that in the case of HepG2 cells, a kind of apoptosis has been induced.

HepG2 cells which were incubated with Photofrin® and irradiated in the absence of UDCA did show enhanced DNA-laddering, whereas in the presence of UDCA laddering was not different from controls. The reason for this somewhat unexpected finding might be that Photofrin® in combination with UDCA pushes PDT more into the direction of necrosis and hence diminishing the proportion of apoptosis. This is consistent with the findings previously reported,[38] where UDCA potentiated CDCA cytotoxicity through necrotic cell death, deduced from enhanced cytochrome *c* release but absence of DNA-fragmentation and activation of caspase-9, all similar to our results. From SLIM we can conclude that the mitochondrial membrane was disturbed when HepG2 cells were treated with Photofrin® in presence of UDCA. This was concluded from the long fluorescence lifetime of most flavine molecules (spectral range 508–520 nm, see Table 1), which seems to be typical for situations where the respiratory chain is deficient[34] and augmented unbound isoalloxazine is present.[35] This could be the reason for the enhanced cytochrome *c* release that was observed post PDT. In accordance, Castelli *et al.* has proposed that the proapoptotic effect of UDCA is due to the fact that UDCA causes a conformational change in the Bcl-2 protein which promotes the affinity for certain membrane-bound photosensitizers thus enhancing photodamage.[40] Bcl-2 photodamage with unaffected bax protein seems to be the first detectable effect leading to cytochrome *c* release when photosensitizers were applied which localize in cytosolic membranes.[41]

The absence of caspase activation in both cell types suggests that a substantial amount of cells undergo necrotic or different cell death pathways. However caspase activation is as well no imperative prerequisite for apoptosis, as a kind of apoptosis can occur in a programmed fashion but in complete absence and independently of caspase activation because other, non-caspase proteases are able to execute programmed cell death.[42,43] Non-caspase proteases as cathepsins, calpains and granzymes are possible candidates to trigger apoptosis. In the case of Huh7 cells we never observed DNA-fragmentation and enhanced cytochrome *c* release from the mitochondria in contrast to HepG2 cells. However this does not mean that no apoptosis took place at all. Apoptosis can also be accomplished when fragmentation is only performed to the stage of high molecular DNA fragments (stage I) resulting in fragments sized about 50–300 kb,[44] which was not investigated within this study. The reason for the missing of enhanced cytochrome *c* release in our Huh7 cell line might be that the anti-apoptotic protein Bcl-2 is not expressed in some Huh7 cells.[45,46] Possibly the mitochondrial metabolism is different which SLIM analysis suggests where Huh7 cells showed an autofluorescence lifetime similar to that found in respiratory deficient saccharomyces.[36] This could also correlate to the fact that mutation of p53 was reported to affect activity of the respiratory chain. p53 is one of the most frequently mutated genes in human cancers and is involved in the regulation of mitochondrial respiration.[47] Furthermore the mutation of the p53 gene is likely the reason for the fact that our Huh7 cells are less sensitive to PDT regardless whether Photofrin® was used in combination with UDCA or Photofrin® alone, as shown in Fig. 1. This finding is in agreement with the reports of Tong *et al.*[28] who could demonstrate that LSF cells (Li–Fraumeni syndrome) that express only mutant p53 were more resistant to Photofrin®-mediated PDT compared to normal human fibroblasts. Zhang *et al.*[29] could show that the HT29 colorectal carcinoma cell line which bears a mutant p53 was sensitized to PDT by infection with wild-type p53.[47]

It seems, that mitochondrial photodamage is less important in our Huh7 cell line and that apoptotic pathways are not the predominant reason for cell death or are probably not involved at all, although it was demonstrated very recently by Zawacka-Pankau *et al.*[48] that in the case of PPIX-induced PDT both p53-dependent and -independent apoptosis occurred; *e.g.* prevailing necrotic processes could have taken place or autophagy, an alternative death mode after PDT. Kessel and Reiners propose that autophagic death can occur when apoptosis is impaired and cells are not sufficiently damaged to evoke necrosis.[49]

In conclusion, Photofrin®–PDT in the presence of UDCA induced cell death pathways in HepG2 cells *via* perturbation of the mitochondrial membrane. The PDT efficiency was potentiated with UDCA possibly by pushing the death pathways from apoptosis more into the direction of necrosis. For Huh7 cells mitochondrial photodamage was less important and apoptotic pathways might not be involved or were different. This was correlated with a different mitochondrial metabolism by means of SLIM for the two cell lines investigated.

Acknowledgements

This work was carried out with financial support by Axcan Pharma Inc. Research development and implementation of the SLIM technique was supported by the Ministry of Economic Affairs of the state of Baden-Württemberg by means of the Landesstiftung Baden-Württemberg, order 4-4332.62-ILM/15. The authors gratefully acknowledge Frank Dolp for technical assistance with the SLIM technique.

References

1 H. C. Wolfsen, Present status of photodynamic therapy for high-grade dysplasia in Barrett's esophagus, *J. Clin. Gastroeneterol.*, 2005, **39**(3), 189–202.
2 V. R. Litle, J. D. Luketich, N. A. Christie, P. O. Buenaventura, M. Alvelo-Rivera, J. S. McCaughan, N. T. Nguyen and H. C. Fernando, Photodynamic therapy as palliation for esophageal cancer: experience in 215 patients, *Ann. Thorac. Surg.*, 2003, **76**(5), 1687–1692.
3 E. Schenkman and D. L. Lamm, Superficial bladder cancer therapy, *Sci. World J.*, 2004, **28**(4), 387–399.
4 M. A. Ortner, Photodynamic therapy in cholangiocarcinomas, *Best Pract. Res. Clin. Gastroenterol.*, 2004, **18**(1), 147–154.
5 B. U. Jones, M. Helmy, M. Brenner, D. L. Serna, J. Williams, J. C. Chen and J. C. Milliken, Photodynamic therapy for patients with advanced non-small-cell carcinoma of the lung, *Clin. Lung Cancer*, 2001, **3**(1), 37–41.
6 C. J. Gomer, N. Ruker and A. L. Murphree, Differential cell photosensitivity following porphyrin photodynamic therapy, *Cancer Res.*, 1988, **48**, 4539–4542.
7 X. Y. He, R. A. Sikes, S. Thomsen, W. K. Chung and S. L. Jacques, Photodynamic therapy with Photofrin II induces programmed cell death in carcinoma cell lines, *Photochem. Photobiol.*, 1994, **59**, 437–468.
8 K. Takahira, M. Sano, H. Arai and H. Hanai, Apoptosis of gastric cancer cell line MKN45 by photodynamic treatment with Photofrin, *Lasers Med. Sci.*, 2004, **19**, 89–94.
9 M. Dellinger, Apoptosis or necrosis following Photofrin photosensitization: influence of the incubation protocol, *Photochem. Photobiol.*, 1996, **64**, 182–187.
10 C. Fabris, G. Valduga, G. Miotto, L. Borsetto, S. Garbisa and E. Reddi, Photosensitization with zinc(II) phthalocyanine as a switch in the decision between apoptosis and necrosis, *Cancer Res.*, 2001, **61**(20), 7459–7500.

11 P. Agostinis, E. Buytaert, H. Breyssens and N. Hendrickx, Regulatory pathways in photodynamic therapy induced apoptosis, *Photochem. Photobiol. Sci.*, 2004, **3**(8), 721–729.
12 N. L. Oleinick, R. L. Morris and I. Belichenko, The role of apoptosis in response to photodynamic therapy: what, where, why and how, *Photochem. Photobiol. Sci.*, 2002, **1**, 1–21.
13 B. C. Wilson, M. Olivo and G. Singh, Subcellular localization of Photofrin and aminolevulinic acid and photodynamic cross-resistance *in vitro* in radiation-induced fibrosarcoma cells sensitive or resistant to photofrin-mediated photodynamic therapy, *Photochem. Photobiol.*, 1997, **65**, 166–176.
14 D. Kessel, M. Antolovich and K. M. Smith, The role of the Peripheral Benzodiazepine Receptor in the apoptotic response to photodynamic therapy, *Photochem. Photobiol.*, 2001, **74**, 346–349.
15 A. Verma, J. Nye and S. H. Snyder, Characterization of porphyrin interactions with peripheral type benzodiazepine receptors, *Mol. Pharmacol.*, 1988, **34**, 800–805.
16 C. Salet, G. Moreno, F. Ricchelli and P. Bernardi, Singlet oxygen produced by photodynamic action causes inactivation of the mitochondrial permeability transition pore, *J. Biol. Chem.*, 1997, **272**, 21938–21943.
17 F. Ricchielli, G. Jori, S. Gobbo, P. Nikolov and V. Petronilli, Discrimination between two steps in the mitochondrial permeability transition process, *Int. J. Biochem. Cell Biol.*, 2005, **37**(9), 1858–1868.
18 D. Kessel, J. A. Caruso and J. J. Reiners, Jr., Potentiation of Photodynamic Therapy by Ursodeoxycholic Acid, *Cancer Res.*, 2000, **60**, 6985–6988.
19 C. M. Rodrigues and C. J. Steer, The therapeutic effects of ursodeoxycholic acid as an antiapoptotic agent, *Expert Opin. Invest. Drugs*, 2001, **10**(7), 1243–1253.
20 R. E. Poupon, K. D. Lindor, K. Cauch-Dudek, E. R. Dickson, R. Poupon and E. J. Heathcote, Combined analysis of randomized controlled trials of ursodeoxycholic acid in primary biliary cirrhosis, *Gastroenterology*, 1997, **113**, 884–890.
21 C. M. Rodrigues and C. J. Steer, Mitochondrial membrane perturbations in cholestasis, *J. Hepatol.*, 2000, **32**, 135–141.
22 C. M. Rodrigues, X. Ma, C. Linehan-Stieers, G. Fan, B. T. Kren and C. J. Steer, Ursodeoxycholic acid prevents cytochrome *c* release in apoptosis by inhibiting mitochondrial membrane depolarization and channel formation, *Cell Death Differ.*, 1999, **6**, 842–854.
23 G. M. Garbo, M. G. Vicente, V. Fingar and D. Kessel, Effects of ursodeoxycholic acid on photodynamic therapy in a murine tumor model, *Photochem. Photobiol.*, 2003, **78**(4), 407–410.
24 M. Müller, S. Strand, H. Hug, E.-M. Heinemann, H. Walczak, W. J. Hofmann, W. Stremmel, P. H. Krammer and P. R. Galle, Drug-induced apoptosis in hepatoma cells is mediated by the CD95(APO-1/Fas) Receptor/Ligand system and involves activation of wild-type p53, *J. Clin. Invest.*, 1997, **99**(3), 403–413.
25 E. Borenfreund and J. A. Puerner, Toxicity determined in vitro by morphological alterations and neutral red absorption, *Toxicol. Lett.*, 1985, **24**(2–3), 119–124.
26 A. Rück, C. Hülshoff, I. Kinzler, W. Becker and R. Steiner, SLIM: A new method for molecular imaging, *Micr. Res. Techn.*, 2007, **70**, 485–492.
27 W. Becker, Advanced time-correlated single photon counting techniques, *Springer Series in Chemical Physics*, Springer-Verlag, Berlin, Heidelberg, 2005.
28 Z. Tong, G. Singh and A. J. Rainbow, The role of the p53 tumor suppressor in the response of human cells to Photofrin-mediated photodynamic therapy, *Photochem. Photobiol.*, 2000, **71**(2), 201–210.
29 W G Zhang, X W Li, L P Ma, S W Wang, H Y Yang and Z Y Zhang, Wild -type p53 protein potentiates phototoxicity of 2-BA-2-DMHA in HT29 cells expressing endogenous mutant p53, *Cancer Lett.*, 1999, **26**(1–2), 189–195.
30 H. Schneckenburger, K. König, K. Kunzi-Rapp, C. Westphal-Frösch and A. Rück, Time resolved in-vivo fluorescence of photosensitizing porphyrins, *J. Photochem. Photobiol., B*, 1993, **21**, 143–147.
31 K. König, H. Schneckenburger, A. Rück and R. Steiner, *In vivo* photoproduct formation during PDT with ALA-induced endogenous porphyrins, *J. Photochem. Photobiol., B*, 1993, **18**, 287–290.
32 H. Schneckenburger, M. H. Gschwend, R. Sailer, A. Rück and W. S. L. Strauβ, Time-resolved pH dependent fluorescence of hydrophilic porphyrins in solution and in cultivated cells, *J. Photochem. Photobiol., B*, 1995, **27**, 251–255.
33 H. Schneckenburger and K. König, Fluorescence decay kinetics and imaging of NAD(P)H and flavins as metabolic indicators, *Opt. Eng.*, 1992, **31**(7), 1447–1451.
34 D. Schweitzer, M. Hammer, F. Schweitzer, R. Anders, T. Doebbecke, S. Schenke and E. R. Gaillard, *In vivo* measurement of time-resolved autofluorescence at the human fundus, *J. Biomed. Opt.*, 2004, **9**, 1214–1222.
35 H. Schneckenburger, P. Gessler and I. Pavenstädt-Grupp, Measurements of Mitochondrial Deficiencies in Living Cells by Microspectrofluorometriy, *J. Histochem. Cytochem.*, **40**(10), 1573–1578.
36 R. J. Paul and H. Schneckenburger, Oxygen concentration and the oxidation-reduction state of yeast: Determinations of free/bound NADH and Flavins by time-resolved spectroscopy, *Naturwissenschaften*, 1996, **83**, 32–35.
37 C. M. Rodrigues, G. Fan, X. Ma, B. T. Kren and C. J. Steer, A novel role for ursodeoxycholic acid in inhibiting apoptosis by modulating mitochondrial membrane perturbation, *J. Clin. Invest.*, 1998, **101**, 2790–2799.
38 A. P. Rolo, C. M. Palmeira, J. M. Holy and K. B. Wallace, Role of mitochondrial dysfunction in combined bile acid-induced cytotoxicity: The switch between apoptosis and necrosis, *Toxicol. Sci.*, 2004, **79**, 196–204.
39 J. Morgan, W. R. Potter and A. R. Oseroff, Comparison of photodynamic targets in a carcinoma cell line and its mitochondrial DNA-deficient derivative, *Photochem. Photobiol.*, 2000, **71**(6), 747–757.
40 M. Castelli, J J Reiners, Jr. and D. Kessel, A mechanism for the proapoptic activity of ursodeoxycholic acid: effects on Bcl-2 conformation, *Cell Death Differ.*, 2004, **11**, 906–914.
41 D. Kessel and M. Castelli, Evidence that bcl-2 is the target of three photosensitizers that induce a rapid apoptotic response, *Photochem. Photobiol.*, 2001, **74**(2), 318–322.
42 L. E. Bröker, F. A. E. Kruyt and G. Giaccone, Cell death independent of caspases: A review, *Clin. Cancer Res.*, 2005, **11**, 3155–3162.
43 D. E. Johnson, Noncaspase proteases in apoptosis, *Leukemia*, 2000, **14**(9), 1695–1703.
44 F. Oberhammer, J. W. Wilson, C. Dive, I. D. Morris, J. A. Hickman, A. E. Wakeling, P. R. Walker and M. Sikorska, Apoptotic death in epithelial cells: cleavage of DNA to 300 and/or 50 kb fragments prior to or in the absence of internucleosomal fragmentation, *EMBO J.*, 1993, **12**(9), 3679–3684.
45 Y.-L. Huang and C.-K. Chou, Bcl-2 blocks apoptotic signal of transforming growth factor-β in human hepatoma cells, *J. Biomed. Sci.*, 1998, **5**, 185–191.
46 Y. Takeda, K. Nakao, K. Nakata, A. Kawakami, H. Ida, T. Ichikawa, M. Shigeno, Y. Kajiya, K. Hamasaki, A. Kato and K. Eguchi, Geranylgeraniol, an intermediate product in mevalonate pathway, induces apoptotic cell death in human hepatoma cells: death receptor-independent activation of caspase-8 with down-regulation of Bcl-xL expression, *Jpn. J. Cancer Res.*, 2001, **92**(9), 918–925.
47 S. Matoba, J.-G Kang, W. D. Patino, A. Wragg, M. Boehm, O. Gavrilova, P. J. Hurley, F. Bunz and P. M. Hwang, p53 regulates mitochondrial respiration, *Science*, 2006, **312**(5780), 1650–1653.
48 J. Zawacka-Pankau, N. Issaeva, S. Hossain, A. Pramanik, G. Selinova and A. J. Podhajska, Protoporphyrin IX interacts with wild-type p53 protein and induces cell death of human colon cancer cells in a p53-dependent and-independent manner, *J. Biol. Chem.*, 2007, **282**, 2466–2472.
49 D. Kessel and J. J. Reiners, Cell death pathways associated with PDT, *Proc. SPIE*, 2006, **6139**, 613902.

